Probing Quantal Dynamics of Mixed Phase Space Systems with Noise

L. Sirko,[1,2] M. R. W. Bellermann,[2] A. Haffmans,[2] P. M. Koch,[2] and D. Richards[3]

[1]*Institute of Physics, Polish Academy of Sciences, Al. Lotników 32/46, 02-668 Warszawa, Poland*
[2]*Physics Department, State University of New York, Stony Brook, New York 11794-3800*
[3]*Mathematics Faculty, Open University, Milton Keynes, MK7 6AA, England*
(Received 10 March 1993)

We study how weak broadband noise affects 30.36 GHz 10%-"ionization" thresholds $F(10\%)$ (that produce "ionization" probability $P_{ion} = 10\%$) of $n_0 = 54, \ldots, 72$ H atoms. Calculations confirm that increased noise lowers $F(10\%)$ for most n_0's, raises some, but affects others little. We show noise to be a useful spectroscopic tool for uncovering novel quantal phenomena such as scarred states, which we link semiclassically to approximately adiabatic evolution near the separatrix of a nonlinear resonance island. Our results apply generally to the quantal behavior of classical mixed phase space systems.

PACS numbers: 05.45.+b, 03.65.Sq, 32.80.Rm

Classical Hamiltonian dynamics in regions of phase space containing both regular and irregular motion is complicated [1]. Lack of a general theory limits our understanding of the quantal/classical correspondence [2–4] of these *mixed systems,* thereby directing attention to particular systems. For regular systems conventional semiclassical methods may be used [4–6]; for hyperbolic systems trace formulas with unstable periodic orbits (PO) are used to find semiclassical energy level densities [4,7].

Because quantal calculations on mixed systems, which are ubiquitous, are difficult and especially challenging if the continuum is involved, the few extant low-dimensional systems on which experiments and both classical and quantal calculations can be performed are particularly important: Three examples are (i) the quadratic Zeeman effect of H atoms [8], (ii) doubly excited He atoms [9], and (iii) periodically driven H atoms [10–14].

A generic structure in mixed systems is the resonance island where regular and irregular motions meet and coexist: A stable PO is surrounded by invariant curves, themselves surrounded by stable and unstable manifolds; such structures exist at all scales.

When island structures manifest themselves in the quantal dynamics, semiclassical approximations are most enlightening. For a system of N freedoms, an island of volume $V \gg h^N$, h being Planck's constant, contains many quantal states almost entirely within it, and classical and quantal dynamics will be locally similar. If $V \lesssim h^N$, no states will live inside the island, but some orbits can be trapped inside it, so classical and quantal dynamics should be qualitatively different. Surrounding an island are stable and unstable manifolds associated with unstable PO. Though of zero measure in a representative ensemble of classical orbits, unstable POs play a key role in quantal dynamics; anchored to them are scarred wave functions (for short, scars) having an enhanced density where the classical dynamics is least stable. Though most studied for billiards [15], scars have been found in calculations on both autonomous systems: H atoms in a strong magnetic field [16] and doubly excited He atoms [9], and time-dependent systems; the kicked rotor [17] and the periodically driven 1D H atom [18].

Scars are important: Emphasizing regions of phase space where classical distributions are statistical, scars produce important local differences in systems having large actions $I \gg h$. In real systems a high density of states hinders preparation of a particular scarred state because the energy resolution requires long times [19]. We stress that no experimentally realizable system can be totally isolated from its environment (hereafter abbreviated as "noise"). With a high density of states, noise-induced effects become important on a time scale that decreases as the noise level increases [20,21]. In particular, because noise destroys unstable PO, we expect that quantal physical phenomena linked to them will be affected. A consequence will be that as noise increases, scars will cause smaller departures from classical behavior.

In this Letter we test our expectations with experimental and theoretical results on a real system, an excited H atom driven by a harmonic electric field with added noise [22], both linearly polarized. For a range of applied frequencies ω and field amplitudes F_ω, the noise-free classical system has mixed character, and important manifestations of scars have been identified in calculations [12,18] and experimental data [23]. The system is time dependent with two freedoms, but it is known [13,24,25] to be approximated well for F_ω near the onset of "ionization" by a time-dependent, one-freedom system.

Our apparatus has been described previously [23,24, 26,27], so we emphasize only important details. A 14.6 keV beam of H atoms, initially in a uniform distribution of substates with a given principal quantum number $n_0 \in$ [54,72] prepared by laser excitation, traversed a section of Ka band, TE_{10}-mode Cu waveguide, entering and exiting through 0.53 mm diam holes centered in each short side wall. A low-noise synthesized source (Gigatronics model 900) was amplified (Miteq model AFD4-080180-2P) and frequency doubled (Honeywell model A2000N). Its amplified [Hughes model 1077H12F00, 24–40 GHz, 1-W traveling-wave-tube amplifier (TWTA)] output passed through a vacuum window, crossed the atomic beam, and was absorbed in a well-matched waveguide
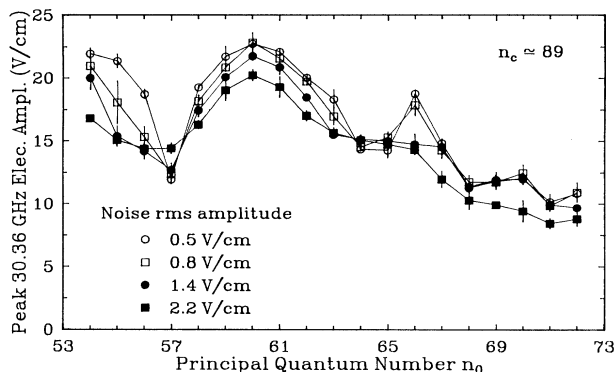
FIG. 1. Measured 10% ionization thresholds vs n_0, for four different rms amplitudes of 26–40 GHz shot noise added to a 30.36 GHz field. Straight lines join data points.
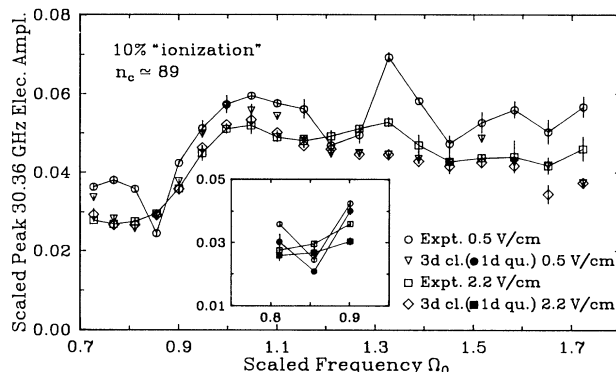

FIG. 2. Comparisons of scaled 10% thresholds vs scaled frequency $n_0^3\omega \equiv \Omega_0$ for two different rms noise amplitudes. Expt: Measurements with 3D atoms, $n_0 = 54, \ldots, 72$; 3d cl: 3D classical Monte Carlo calculations; 1d qu: 1D quantal calculations neglecting the continuum. Straight lines join data points.

load. In a separate experiment in our apparatus we used Stueckelberg oscillations in He Rydberg atoms [26] to calibrate the 30.36 GHz amplitude F_ω to 1%.

This frequency is the same one used previously [23], but note how the experiments differ: (i) (somewhat important) the present (previous) pulse shape is a half sine wave (three-lobes, with the middle lobe) lasting 129 (182) field oscillations; (ii) (very important) the present (previous) waveguide (high-Q cavity) interaction region was used to support (act as few MHz wide filter and suppress) the broadband noise spectrum of the TWTA (flat within 10 dB over 26.5–40 GHz). We assume it was predominantly shot noise (equal quantities of amplitude and phase noise). We used a broadband, variable attenuator after the TWTA to decrease the rms noise amplitude F_n and still vary F_ω, up to a limit set by TWTA saturation. For each n_0 we used the proton quench method to measure P_{ion} as a function of F_ω, for each of four different F_n values; "ionization" means true ionization plus excitation above an n cutoff, $n_c^q \simeq 89$ [27].

The 10% thresholds $F(10\%)$ in Fig. 1 show the effect of noise to be neither uniform nor systematic as n_0 varies: (i) At the lower two F_n values the $F(10\%)$ for each n_0 are usually close, *except* especially for $n_0 = 55$ and 56. (ii) Increased noise usually decreases $F(10\%)$ (increases P_{ion}). (iii) That the counterexamples to (ii), $n_0 = 57$ and 65, occur at local minima in $F(10\%)$ suggests a qualitative explanation. At such a minimum the (atom + field) wave function must be dominated by relatively unstable Floquet states, so (weak) noise can only mix in nearby more stable states. (iv) In one case, $n_0 = 64$ (see also $n_0 = 68$), noise has little influence. This suggests either that noise-induced coupling to other Floquet states is weak here or that whatever Floquet state(s) are mixed in become unstable against ionization near $F_\omega = 15$ V/cm.

The (i)–(iv) behavior is in stark contrast with that measured [21] for Rb Rydberg atoms with *ratios* of F_n/F_ω comparable to those we used for H. For *all* Rb data shown in Fig. 1 of [21], $F(10\%)$ systematically *de-*

creases as F_n increases.

We focus now on H($n_0 = 66$). A previous low-noise 30.36 GHz experiment [23] found it to be an example of nonclassical local stability (non-CLS) that scales classically, being associated with the scaled frequency $\Omega_0 \simeq 1.3$. In Fig. 1 the local stability of $n_0 = 66$ stands out for $F_n = 0.5$ and 0.8 V/cm but is almost completely destroyed when $F_n \geq 1.4$ V/cm. In a 1D model of the driven atom, the non-CLS was identified numerically with a region of phase space near an unstable PO [12,18]. Our data are consistent with this identification, showing whatever stabilizes this state is sensitive to noise, as would be expected for an unstable PO. Why noise similarly affects $n_0 = 55$ and 56 will be explained below.

Henceforth we use atomic units with the scaled amplitude $n_0^4 F$ and frequency $\Omega_0 \equiv n_0^3\omega$ [28]. Figure 2 compares $F(10\%)$ data with 3D classical Monte Carlo calculations (3D MC), which used the method described in [27], but now with added noise modeled as random telegraph phase noise [29]. The Hamiltonian (see [14]) is $\mathcal{H}(t) = \mathbf{p}^2/2 - 1/r + (F_\omega/\omega)p_z A(t)\sin[\omega t + \varphi(t)]$, where $A(t)$ is the experimental pulse shape, and $\varphi(t)$ jumps between a certain $\pm \Delta\varphi$ at random times t_k, with $t_{k+1} - t_k$ exponentially distributed with a mean λ^{-1}. After determining for the experimental $A(t)$ that the results were insensitive to quite large changes in λ^{-1}, we chose it to be $4\pi/\omega$. In this model $F_n = F_\omega \sqrt{2} \sin\Delta\varphi$.

For $F_n = 0.5$ V/cm ($\Delta\varphi/\pi$ between 0.005 and 0.01), Fig. 2 shows agreement within combined experimental and 3D MC statistical errors in only 4 of 19 cases; significant differences are at $n_0 = 55$, 56, 63, 66, 67, and 70–72. Separate 3D MC for $F_n = 0$, not shown here, were generally indistinguishable from the present 3D MC with $F_n = 0.5$ V/cm.

For $F_n = 2.2$ V/cm ($\Delta\varphi/\pi$ between 0.025 and 0.055), Fig. 2 shows excellent agreement in 14 out of 19 cases: Ω_0 between 0.72 and 1.15 and between 1.45 and 1.58.

Between 1.21 and 1.39 and between 1.65 and 1.72, the differences are similar to but smaller than those for F_n =0.5 V/cm.

Dramatically opposite to n_0=66 (and 55,56) is n_0=57, where noise *increases* $F(10\%)$. Figure 2 (inset) compares 3D atom data for n_0=56–58 with 1D numerical integrations of the Schrödinger equation in the dipole gauge, with the field modeled as $A(t)\{F_\omega \sin\omega t + [F_n/ (\sum_{k=1}^{20} a_k^2)^{1/2}]\sum_{k=1}^{20} a_k \sin(2\pi \nu_k t + \varphi_k)\}$. Defining ionization as excitation to $n \geq 90$ in the $n \in [50,170]$ basis of zero-field states, we took experimental values for ω, F_n, and $A(t)$ and a_k, φ_k, and ν_k to be uniformly distributed on [0,1], [0,2π], and [22,40] GHz, respectively. Averaged over five independent noise realizations, the calculations reproduce the measured behavior very well.

We also included the continuum in 1D quantal calculations, using semiclassical methods [14] and a random phase noise model [29]. (For the present noise levels, random phase and random amplitude noise models gave insignificantly different results.) Because the method adds a static field term $-zF_s$ to $\mathcal{H}(t)$ to "lower the continuum" to a *saddle* n-value n_s, one should compare the results only qualitatively to the present experiment, in which F_s =0. Figure 3 shows for n_0=66, $n_0^4 F$ =0.05, F_s =8 V/cm (giving n_s =95), and λ^{-1}=2π/ω how P_{ion} varies with the F_s-shifted scaled frequency $\Omega_1 = \Omega_0(1 + 3n_0^4 F_s)$ [30] as $\Delta\varphi$ and, thus, F_n increase. At local minima P_{ion} increases with F_n, but most dramatically in a range around Ω_1 =1.32, just where the present experiment (Ω_0 =1.327 for n_0=66) shows strong noise-induced destabilization [lowering of $F(10\%)$]. Figure 3 also shows cases of noise-induced stabilization near local maxima in P_{ion} and other cases where added noise has little effect [cf. behaviors (iii) and (iv) above].

Though the nonconstant $A(t)$ complicates an analytic understanding of our results, it varies slowly enough for adiabatic invariance to give powerful insight into the dy-
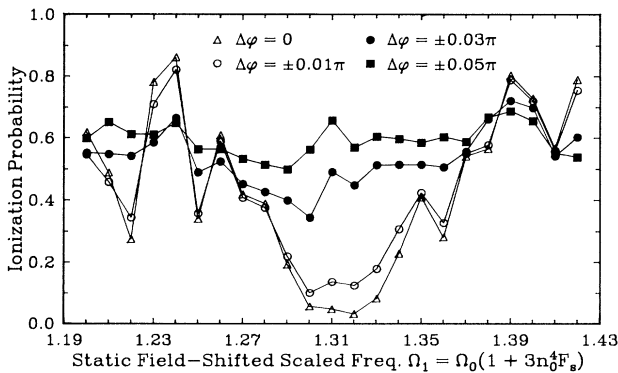
FIG. 3. 1D quantal calculations that included the continuum, for n_0=66 in a microwave (peak amplitude $n_0^4 F$ =0.05) and static fields (F_s =8 V/cm) with added random telegraph phase noise having the indicated fixed phase jumps. Straight lines join points in each set.

namics. A key point is that when P_{ion} =10%, even the peak ionization rate is low. Use of a 1D model H atom will be sufficiently accurate near the onset of ionization [12,13,24,25].

As is customary near a resonance, we express the bound-motion Hamiltonian $\mathcal{H}$ in unperturbed action-angle variables (I,θ), expand about the resonant action $I_r = \Omega^{-1/3}$, and transform to a frame rotating at frequency Ω to remove slowly varying terms [1] to give $\mathcal{H} = \mathcal{H}_p + \mathcal{H}_1$. (For the equivalent quantal procedure, see [31]). The "pendulum" Hamiltonian $\mathcal{H}_p$ describes motion near the resonance, see [32], $\mathcal{H}_p = -3X^2/2I_r^4 + 2X^3/I_r^5 + 0.325FA(t)I_r^2\cos\theta$, with $I = I_r + X$. The small X^3 term is qualitatively unimportant but affects details discussed below. The Hamiltonian $\mathcal{H}_1$ contains relatively rapid terms such as $\exp \pm i(\theta + 2\Omega t)$ and $\exp \pm i[s\theta + (s \pm 1)\Omega t]$, for $s \geq 2$.

When $A(t)$ =1, $\mathcal{H}_p$ has a stable [unstable] fixed point at (0,0) [(0, $\pm\pi$)], corresponding to stable (unstable) POs in the original representation. The separatrix associated with the unstable fixed point has energy $E_s = -0.325FI_r^2$; its area encloses about N_s quantal states, where N_s =0.84$I_r\sqrt{F_r}/\hbar$, for $F_r = FI_r^4$. The frequency of motion near the stable fixed point is ω_p =0.98$F_r^{1/2}\Omega$. For present parameters $N_s \simeq 10$ and $\omega_p \simeq 0.23\Omega$.

Near the Ω_0=1 resonance the eigenstates of $\mathcal{H}_p$ are the natural quantal basis; without the X^3 term, they are the even ce_{2r} and odd se_{2r}, r=0,1,..., Mathieu functions [33] with argument $v = (\theta + \pi)/2$.

If $\mathcal{H}_1$ were zero, for $A(t)$ slow enough each initial state $\exp(ip\theta)/\sqrt{2\pi}$, $p = \pm r$, is, because of parity, transformed adiabatically into linear combinations of the pair ce_{2r} and se_{2r} in roughly equal weights. The resonant state p =0 is an exception: It becomes the ground state ce_0. $dA(t)/dt$ controls the purity of this transformation, with faster rates tolerated as $|p|$ increases; for present experimental conditions $A(t)$ is indeed slow. The nonzero $\mathcal{H}_1$ mixes these adiabatic states. "Ionization," which is due to mixing with states of large n, is complicated because it depends on the size of matrix elements and time scales. Here we are interested only in the gross features of the dynamics, which depend on which state(s) of $\mathcal{H}_p$ are populated by the slowly varying $A(t)$.

To find these states we use classical adiabatic invariance. Rigorously it breaks down because of the potential barrier at $\theta = \pm \pi$, but because this affects only a few orbits, the initial and final actions for most orbits in an ensemble have similar magnitude.

For N_s large enough, the highest energy states of $\mathcal{H}_p$, with $E_m \simeq (m + \frac{1}{2})\hbar\omega_p$, m =0,1,..., resemble those of a linear oscillator: They are localized near θ =0, with little support outside the separatrix, and because ω_p is relatively small these states are only weakly perturbed by $\mathcal{H}_1$ so, once populated, require a strong field to be ionized. This accounts for the broad maximum in Figs. 1 and 2 centered at n_0=60, $\Omega_0 \simeq 1$ [34].

Eigenstates with energy near E_s are peaked near

$\theta = \pm \pi$, where classical motion is slowest. Moreover, results presented elsewhere [34] show that one of the states near the separatrix is perturbed less by $\mathcal{H}_1$ than are adjacent states. Though not obvious from the form of $\mathcal{H}_p$, this local quantal stability is related to the large classical period near the separatrix and accounts for the local maximum in Figs. 1 and 2 at $n_0 = 66$, $\Omega_0 \simeq 1.3$.

A separatrix (scarred) state can be populated by starting the system with $A(t) = 0$ in a rotational state having quantum numbers $X \simeq \pm N_s/2$, i.e., starting above or below the resonant state with a classical action about half the separatrix area. Because $\mathcal{H}_p$ is asymmetric about $X = 0$, to create a separatrix state requires starting with actions $I_s^{\pm}$ asymmetrically placed about I_r. Computing relevant areas gives $I_s^{\pm} = (1 \pm 0.419\sqrt{F_r} + 0.144 F_r + \cdots) I_r$. Parity conservation and quantization mean that the quantum numbers of those initial states evolving into scarred states are within an integer of $I_s^{\pm}$; Ref. [34] gives the explicit derivation. Initial actions within $I_s^- < I < I_s^+$ will populate (librational) states [34,35] predominantly in the island interior. For a 30.36 GHz field, $I_r = 60.1$; at $F_0(10\%) = 0.0692$ for $n_0 = 66$ in Fig. 2, $F_r = 0.0473$. These values give $I_s^+ = 65.9$ and $I_s^- = 55.0$, which agree excellently with the data in Fig. 1. A separatrix (scarred) state is populated from $n_0 = 66$ and 55,56: In Fig. 1, at $F_n = 0.5$ V/cm, $F(10\%)$ for $n_0 = 56$ and 66 are the same in V/cm, and $n_0 = 55,56,66$ are all examples of non-CLS that are particularly sensitive to noise, which evidently mixes in less stable, nearby states.

The present Letter deals with a particular system, the H atom driven by a strong microwave field. Experimental and theoretical results showed the effect of added noise to be neither uniform nor systematic, but, remarkably, it can be used as a *spectroscopic tool* to aid in uncovering novel quantal phenomena. We expect our results will be generally applicable for unraveling the quantal behavior of other mixed phase space Hamiltonian systems, which are ubiquitous in nature.

[1] A. J. Lichtenberg and M. A. Lieberman, *Regular and Stochastic Motion* (Springer, New York, 1983); B. V. Chirikov, Phys. Rep. **52**, 263 (1979).

[2] See papers in *Irregular Atomic Systems and Quantum Chaos*, edited by J.-C. Gay [Comments At. Mol. Phys. **25**, Nos. 1-6 (1990-1991)].

[3] See papers in *Chaos and Quantum Physics*, edited by M.-J. Giannoni, A. Voros, and J. Zinn-Justin (Elsevier, Amsterdam, 1991).

[4] M. C. Gutzwiller, *Chaos in Classical and Quantum Mechanics* (Springer, New York, 1990).

[5] I. C. Percival, Adv. Chem. Phys. **36**, 1 (1977).

[6] I. C. Percival and D. Richards, Adv. Atm. Mol. Phys. **11**,

[7] See papers on periodic orbit theory in Chaos **2** (1992).

[8] H. Friedrich and D. Wintgen, Phys. Rep. **183**, 37 (1989); J. Main, G. Wiebusch, and K. H. Welge, in *Irregular Atomic Systems and Quantum Chaos* (Ref. [2]); D. Delande, in *Chaos and Quantum Physics* (Ref. [3]); C.-h. Iu *et al.*, Phys. Rev. Lett. **66**, 145 (1991).

[9] D. Wintgen, K. Richter, and G. Tanner, in [7].

[10] J. E. Bayfield and P. M. Koch, Phys. Rev. Lett. **33**, 258 (1974).

[11] G. Casati, I. Guarneri, and D. L. Shepelyansky, IEEE J. Quantum Electron. **24**, 1420 (1988).

[12] R. V. Jensen, S. M. Susskind, and M. M. Sanders, Phys. Rep. **201**, 1 (1991).

[13] L. Moorman and P. M. Koch, in *Quantum Nonintegrability*, edited by D. H. Feng and J.-M. Yuan (World Scientific, Singapore, 1992), pp. 142-243.

[14] J. G. Leopold and D. Richards, J. Phys. B **24**, 1209 (1991).

[15] R. Blümel *et al.*, Phys. Rev. A **45**, 2641 (1992); S. Sridhar and E. J. Heller, *ibid.* **46**, R1728 (1992), and references therein.

[16] D. Delande and J.-C. Gay, Phys. Rev. Lett. **59**, 1809 (1987); D. Wintgen and A. Hönig, *ibid.* **63**, 1467 (1989).

[17] G. Radons and R. E. Prange, Phys. Rev. Lett. **61**, 1691 (1988); in *Quantum Chaos*, edited by H. A. Cerdeira *et al.* (World Scientific, Singapore, 1991).

[18] R. V. Jensen *et al.*, Phys. Rev. Lett. **63**, 2771 (1989).

[19] M. Berry, in *Chaos and Quantum Physics* (Ref. [3]) stresses the noninterchangeability of the $\hbar \to 0$ and $t \to \infty$ limits in semiclassical treatment of classically chaotic systems.

[20] R. Blümel *et al.*, Phys. Rev. A **44**, 4521 (1991).

[21] M. Arndt *et al.*, Phys. Rev. Lett. **67**, 2435 (1991).

[22] J. E. Bayfield, Chaos **1**, 110 (1991).

[23] B. E. Sauer, M. R. W. Bellermann, and P. M. Koch, Phys. Rev. Lett. **68**, 1633 (1992); P. M. Koch, in [7].

[24] P. M. Koch *et al.*, Phys. Scr. **T26**, 51 (1989).

[25] The absence of calculated scar-induced local stability near $\Omega_0 = 1.3$ and 0.8 in A. Buchleitner and D. Delande, Phys. Rev. Lett. **70**, 33 (1993), is a consequence of their neglect of the slow amplitude envelope function $A(t)$.

[26] S. Yoakum, L. Sirko, and P. M. Koch, Phys. Rev. Lett. **69**, 1919 (1992).

[27] E. J. Galvez *et al.*, Phys. Rev. Lett. **61**, 2011 (1988).

[28] J. G. Leopold and I. C. Percival, J. Phys. B **12**, 709 (1979).

[29] J. G. Leopold and D. Richards, J. Phys. B **24**, L243 (1991).

[30] K. Dietz, J. Henkel, and M. Holthaus, Phys. Rev. A **45**, 4960 (1992), Eq. (3.7).

[31] G. M. Zaslavsky, Phys. Rep. **80**, 157 (1981), Sec. 9.1.

[32] I. C. Percival and D. Richards, *Introduction to Dynamics* (Cambridge Univ. Press, Cambridge, 1982).

[33] M. Abramowitz and I. A. Stegun, *Handbook of Mathematical Functions* (Dover, New York, 1964).

[34] The more complicated behavior of the librational states with energies $-E_s < E < E_s$ is dealt with in J. G. Leopold and D. Richards (to be published).

[35] R. V. Jensen, in "Quantum Dynamics of Chaotic Systems," edited by J.-M. Yuan, D. H. Feng, and G. M. Zaslavsky (Gordon and Breach, Langhorne, PA, 1993).